

Chain Complexes of Rhodium(II) Pivalate Dimers Formed by Ligation of C=C Double Bond and Carbonyl Oxygen of *p*-Quinone
 $[\{\text{Rh}_2(\text{O}_2\text{CCMe}_3)_4(p\text{-Q})_2\}\{\text{Rh}_2(\text{O}_2\text{CCMe}_3)_4\}]_n$,
p-Q = 1,4-Benzoquinone and 1,4-Naphthoquinone

Makoto Handa,^{*,1a} Tadahiro Nakao,^{1a}
 Masahiro Mikuriya,^{*,1b} Takanori Kotera,^{1b}
 Ryoji Nukada,^{1b} and Kuninobu Kasuga^{1a}

Department of Material Science, Interdisciplinary Faculty of Science and Engineering, Shimane University, Nishikawatsu, Matsue 690, Japan, and Department of Chemistry, School of Science, Kwansei Gakuin University, Uegahara, Nishinomiya 662, Japan

Received February 28, 1997

Introduction

Tetrakis(μ -carboxylato)dimetal complexes ($\text{M}_2(\text{O}_2\text{CR})_4\text{X}_m$; M = Cr, Mo, W, Tc, Re, Ru, Os, Rh, etc., $m = 0-2$) have been studied extensively from the standpoint of the unique properties conferred by the direct metal–metal bonds within their molecules.² Recently, there have been a number of investigations into the use of the dimetal complexes as building blocks in combination with the ligands of organic acceptors such as tetracyanoethylene (TCNE) and 7,7,8,8-tetracyanoquinodimethane (TCNQ) to produce hybrid donor/acceptor polymers incorporating metal–metal bonds.³ We have been engaged in preparing chain complexes with alternated alignment of the M_2 dimers and a kind of organic acceptor *p*-quinone formed by the axial coordination of the carbonyl oxygens to $\text{M}_2(\text{O}_2\text{CCF}_3)_4$ (M = Mo^{II} and Rh^{II}).⁴ In the previous paper, we reported the chain complexes $[\text{Rh}_2(\text{O}_2\text{CCF}_3)_4(p\text{-Q})]_n$ (*p*-Q = *p*-quinone: 1,4-benzoquinone (1,4-bq), 1,4-naphthoquinone (1,4-nq), and 2,3-dimethyl-1,4-benzoquinone) in which the *p*-quinones link the Rh₂ dimers by their carbonyl groups.^{4c} We have since been interested in the effect of changing the substituent group R of the Rh₂(O₂CR) dimer on the chain structure. By employing Rh₂(O₂CCMe₃)₄, we have found a novel coordination of the C=C double bond of the quinone to the Rh₂ dimer. Here, we present the crystal structures and properties of the chain complexes $[\{\text{Rh}_2(\text{O}_2\text{CCMe}_3)_4(p\text{-Q})_2\}\{\text{Rh}_2(\text{O}_2\text{CCMe}_3)_4\}]_n$ (*p*-Q = 1,4-bq and 1,4-nq). A preliminary report has been published for $[\{\text{Rh}_2(\text{O}_2\text{CCMe}_3)_4(1,4\text{-bq})_2\}\{\text{Rh}_2(\text{O}_2\text{CCMe}_3)_4\}]_n$.⁵

* Address correspondence to M. Handa (fax, +81 (852) 32-6429; e-mail, handam@riko.shimane-u.ac.jp) or to M. Mikuriya (fax, +81 (798) 51-0914; e-mail, junpei@kwansei.ac.jp).

- (1) (a) Shimane University. (b) Kwansei Gakuin University.
- (2) Cotton, F. A.; Walton, R. A. *Multiple Bonds between Metal Atoms*, 2nd ed.; Oxford University Press: New York, 1993.
- (3) (a) Cotton, F. A.; Kim, Y. *J. Am. Chem. Soc.* **1993**, *115*, 8511. (b) Cotton, F. A.; Kim, Y.; Lu, J. *Inorg. Chim. Acta* **1994**, *221*, 1. (c) Ouyang, X.; Campana, C.; Dunbar, K. R. *Inorg. Chem.* **1996**, *35*, 7188. (d) Campana, C.; Dunbar, K. R.; Ouyang, X. *J. Chem. Soc., Chem. Commun.* **1996**, 2427.
- (4) (a) Handa, M.; Sono, H.; Kasamatsu, K.; Kasuga, K.; Mikuriya, M.; Ikenoue, S. *Chem. Lett.* **1992**, 453. (b) Handa, M.; Matsumoto, H.; Namura, T.; Nagaoka, T.; Kasuga, K.; Mikuriya, M.; Kotera, T.; Nukada, R. *Chem. Lett.* **1995**, 903. (c) Handa, M.; Mikuriya, M.; Sato, Y.; Kotera, T.; Nukada, R.; Yoshioka, D.; Kasuga, K. *Bull. Chem. Soc. Jpn.* **1996**, *69*, 3483.
- (5) Handa, M.; Takata, A.; Nakao, T.; Kasuga, K.; Mikuriya, M.; Kotera, T. *Chem. Lett.* **1992**, 2085.

Table 1. Crystal Data and Data Collection Details

	1	2
empirical formula	Rh ₂ O ₁₀ C ₂₆ H ₄₀	Rh ₂ O ₁₀ C ₃₀ H ₄₂
fw	718.41	768.47
cryst syst	triclinic	triclinic
space group	<i>P</i> 1	<i>P</i> 1
<i>a</i> /Å	11.745(5)	10.973(5)
<i>b</i> /Å	15.164(7)	12.037(4)
<i>c</i> /Å	9.862(4)	14.112(9)
α /deg	101.52(2)	73.19(4)
β /deg	98.91(2)	76.12(4)
γ /deg	110.25(3)	73.59(3)
$V/\text{Å}^3$	1565.9(12)	1686.0(15)
<i>Z</i>	2	2
$D_c/\text{g cm}^{-3}$	1.52	1.52
$D_m/\text{g cm}^{-3}$	1.55	1.48
cryst size/mm	0.35 × 0.30 × 0.20	0.65 × 0.38 × 0.30
$\mu(\text{Mo K}\alpha)/\text{cm}^{-1}$	10.8	10.1
2θ range/deg	1.0–48.0	1.0–48.0
no. of reflns measd	4892	5266
no. of unique reflns	3956	4231
with $I > 3\sigma(I)$		
<i>R</i>	0.026	0.056
<i>R_w</i>	0.032	0.070

Experimental Section

Synthesis of $[\{\text{Rh}_2(\text{O}_2\text{CCMe}_3)_4(1,4\text{-bq})_2\}\{\text{Rh}_2(\text{O}_2\text{CCMe}_3)_4\}]_n$ (1). A solution of 1,4-bq (10 mg, 0.09 mmol) in hexane (10 mL) was added to a solution of Rh₂(O₂CCMe₃)₄ (50 mg, 0.08 mmol) in hexane (10 mL) under Ar, and the mixture was stirred for 5 h at room temperature. The precipitate was filtered off, washed with hexane, and dried under vacuum to give a blackish violet powder. The yield was 90% based on Rh₂(O₂CCMe₃)₄. Found: C, 43.73; H, 5.56. Calcd for C₁₃H₂₀RhO₅: C, 43.47; H, 5.61. IR (in KBr) ν/cm^{-1} : $\nu(\text{CO})$ for 1,4-bq, 1630 (m) and 1660 (m); $\nu(\text{COO})$ for [−]O₂CCMe₃, 1420 (s) and 1580 (s).

Synthesis of $[\{\text{Rh}_2(\text{O}_2\text{CCMe}_3)_4(1,4\text{-nq})_2\}\{\text{Rh}_2(\text{O}_2\text{CCMe}_3)_4\}]_n$ (2). This compound was obtained as a brown powder by the reaction of Rh₂(O₂CCMe₃)₄ (50 mg, 0.08 mmol) with 1,4-nq (14 mg, 0.09 mmol) in hexane using a method similar to that of 1. The yield was 90% based on Rh₂(O₂CCMe₃)₄. Found: C, 46.57; H, 5.46. Calcd for C₁₅H₂₁RhO₅: C, 46.89; H, 5.51. IR (in KBr) ν/cm^{-1} : $\nu(\text{CO})$ for 1,4-nq, 1630 (m) and 1670 (m); $\nu(\text{COO})$ for [−]O₂CCMe₃, 1420 (s) and 1580 (s).

Measurements. Elemental analyses for carbon and hydrogen were carried out using a Yanako CHN CORDER MT-5. Electronic spectra and infrared spectra (KBr pellets) were measured with Shimadzu UV-3100 and Hitachi 260-50 spectrometers, respectively. NMR spectra were recorded using a JEOL-GX 270 spectrometer at 270 MHz. The chemical shifts were determined in ppm using TMS as the internal standard. Cyclic voltammograms were obtained with a Hokuto Denko HA-501 potentiostat and an HB-104 function generator using a glassy carbon disk working electrode (3 mm diameter), a Pt coil counter, and a saturated calomel reference electrode (SCE). The concentration values for the complexes were based on the mole amounts of Rh₂(O₂CCMe₃)₄ in the solutions.

X-ray Crystal Structure Analysis. Diffraction data were collected on an Enraf-Nonius CAD4 diffractometer using graphite-monochromated Mo K α radiation at 25 ± 1 °C. Crystal data and details concerning data collection are given in Table 1. The lattice constants were determined by a least-squares refinement based on 25 reflections with 20 ≤ 2 θ ≤ 30°. The intensity data were corrected for Lorentz–polarization effects. The structures were solved by the heavy-atom methods. Refinements were carried out by the full-matrix least-squares methods. All of the non-hydrogen atoms were refined with anisotropic thermal parameters. The methyl carbon atoms on a *tert*-butyl group

- (6) Rh₂(O₂CCMe₃)₄·2H₂O was prepared by a literature method described in ref 8. The water molecules were removed by heating under vacuum.

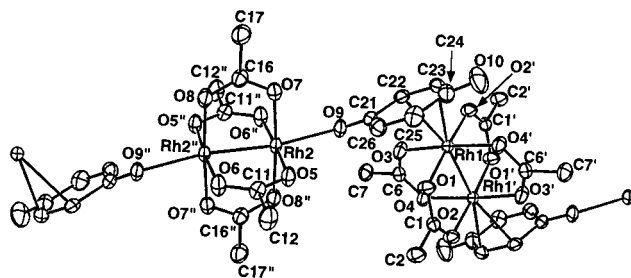


Figure 1. ORTEP drawing of **1**. Hydrogen atoms and CH₃ groups of the pivalate ions are omitted for clarity.

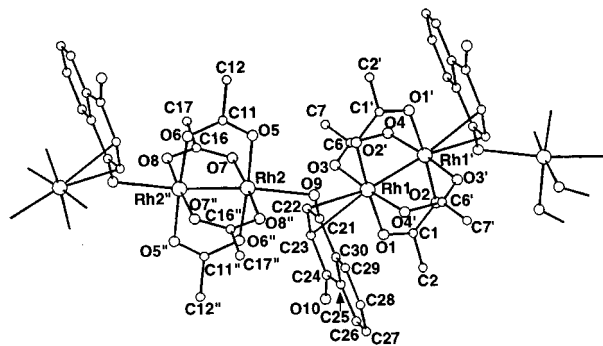


Figure 2. PLUTO drawing of **2**. Hydrogen atoms and CH₃ groups of the pivalate ions are omitted for clarity.

of pivalate for **1** were included in the full-matrix refinement with a disordered model. Hydrogen atoms were fixed at their calculated positions. The weighting scheme, $w = 1/[\sigma^2(|F_o|) + (0.02|F_o|)^2 + 1.0]$, was employed. The final discrepancy factors, $R = \sum ||F_o| - |F_c|| / \sum |F_o|$ and $R_w = [\sum w(|F_o| - |F_c|)^2 / \sum |F_o|^2]^{1/2}$, are listed in Table 1. All of the calculations were carried out on a micro VAX station 4000 90A computer using a MolEN program package.⁷

Results and Discussion

The crystal structures of **1** and **2** are shown in Figures 1 and 2, respectively. The chain structures are formed by alternated arrangement of Rh₂ dimers and *p*-quinone molecules (1,4-bq and 1,4-nq). It should be noted that *p*-quinone is coordinated to the Rh₂ dimer with the C=C double bond as well as the carbonyl oxygen. This coordination mode of *p*-quinone is different from that of the previously reported chain complexes [M₂(O₂CCF₃)₄(*p*-Q)]_n (M = Mo^{II} and Rh^{II}, *p*-Q = 1,4-bq, 1,4-nq, 2,3-dimethyl-1,4-benzoquinone, 2,6-dimethyl-1,4-benzoquinone, and 9,10-antraquinone), in which only the two carbonyl oxygens participate in axial coordination.⁴

The bond distances and angles for the Rh₂ skeleton for **1** and **2** are listed in Table 2. In the case of **1**, a carbonyl oxygen of 1,4-bq is coordinated to the Rh₂ core with a distance of 2.293(2) Å. This value is 0.045 Å larger than the distance for [Rh₂(O₂CCF₃)₄(1,4-bq)]_n^{4c} and almost comparable to the axial Rh—O distance observed for Rh₂(O₂CCMe₃)₄(H₂O)₂ (2.295(2) Å).⁸ The other carbonyl oxygen of 1,4-bq does not participate in the coordination. Rather, a C=C double bond of 1,4-bq is coordinated to the neighboring Rh₂ dimer with Rh—C distances of 2.435(4) and 2.486(5) Å. Such a crystallographically recognized coordination of a C=C double bond to an Rh₂ dimer has been reported only for the compound Rh₂(O₂CCF₃)₄((-)-*trans*-caryophyllene)₂.⁹ The Rh—C distances were 2.46(1),

Table 2. Selected Bond Distances (Å) and Angles (deg) Concerning Rh₂ Cores for **1** and **2** with Their Estimated Standard Deviations in Parentheses

Compound 1 ^a			
Rh1—Rh1'	2.3996(4)	Rh2—Rh2''	2.3768(4)
Rh1—O1	2.020(3)	Rh2—O5	2.029(3)
Rh1—O2'	2.033(3)	Rh2—O6''	2.026(4)
Rh1—O3	2.024(3)	Rh2—O7	2.020(3)
Rh1—O4'	2.028(3)	Rh2—O8''	2.045(3)
Rh1—C22	2.435(4)	Rh2—O9	2.293(2)
Rh1—C23	2.486(5)		
O1—Rh1—O2'	175.3(1)	O6''—Rh2—O7	90.3(1)
O1—Rh1—O3	92.0(1)	O6''—Rh2—O8''	90.2(1)
O1—Rh1—O4'	88.5(1)	O6''—Rh2—O9	86.1(1)
O2'—Rh1—O3	87.8(1)	O7—Rh2—O8''	176.3(1)
O2'—Rh1—O4'	91.3(1)	O7—Rh2—O9	85.5(1)
O3—Rh1—O4'	175.0(1)	O8''—Rh2—O9	98.2(1)
O5—Rh2—O6''	176.4(1)	Rh1'—Rh1—C22	162.1(1)
O5—Rh2—O7	89.7(1)	Rh1'—Rh1—C23	165.9(1)
O5—Rh2—O8''	89.5(1)	Rh2''—Rh2—O9	171.9(1)
O5—Rh2—O9	97.6(1)	Rh2—O9—C21	133.4(3)
Compound 2 ^b			
Rh1—Rh1'	2.402(1)	Rh2—Rh2''	2.367(1)
Rh1—O1	2.013(7)	Rh2—O5	2.035(6)
Rh1—O2'	2.020(7)	Rh2—O6''	2.036(6)
Rh1—O3	2.012(9)	Rh2—O7	2.010(8)
Rh1—O4'	2.028(9)	Rh2—O8''	2.019(8)
Rh1—C22	2.486(8)	Rh2—O9	2.338(7)
Rh2—C23	2.479(9)		
O1—Rh1—O2'	175.0(2)	O6''—Rh2—O7	91.5(3)
O1—Rh1—O3	91.2(3)	O6''—Rh2—O8''	87.7(3)
O1—Rh1—O4'	89.2(3)	O6''—Rh2—O9	85.8(3)
O2'—Rh1—O3	88.8(3)	O7—Rh2—O8''	176.6(3)
O2'—Rh1—O4'	90.5(3)	O7—Rh2—O9	95.7(3)
O3—Rh1—O4'	175.4(2)	O8''—Rh2—O9	87.5(3)
O5—Rh2—O6''	176.6(3)	Rh1'—Rh1—C22	164.2(2)
O5—Rh2—O7	88.2(3)	Rh1'—Rh1—C23	162.8(3)
O5—Rh2—O8''	92.3(3)	Rh2''—Rh2—O9	173.1(2)
O5—Rh2—O9	97.6(2)	Rh2—O9—C21	113.2(6)

^a Primes and double primes refer to the equivalent positions ($-x, -y, -z$) and ($1-x, 1-y, 1-z$), respectively. ^b Primes and double primes refer to the equivalent positions ($-x, -y, 1-z$) and ($1-x, -y, -z$), respectively.

2.62(1), and 2.63(1) Å.⁹ The first value is comparable to those for **1**.

In the case of **2**, the carbonyl oxygen is coordinated to the dimer core (designated as Rh2—Rh2'') with a distance of 2.338(7) Å, while the other Rh₂ unit (designated as Rh1—Rh1') is axially coordinated by C=C double bonds with Rh—C distances of 2.486(8) and 2.479(9) Å.

The Rh—Rh bond distances of **1** and **2** in the oxygen-coordinated Rh₂ cores are almost comparable to that of Rh₂(O₂-CCMe₃)₄(H₂O)₂ (2.371(1) Å).⁸ However, the Rh—Rh distances of the Rh₂ core with the C=C double bonds at their axial positions are ca. 0.03 Å longer than that for Rh₂(O₂CCMe₃)₄(H₂O)₂.⁸

In Table 3, bond distances for *p*-quinone moieties are listed with the data for the free 1,4-bq and 1,4-nq molecules.¹⁰ It is clearly shown that the C=C double bond is lengthened on coordination, though without any accompanying significant difference in C=O bond distance.

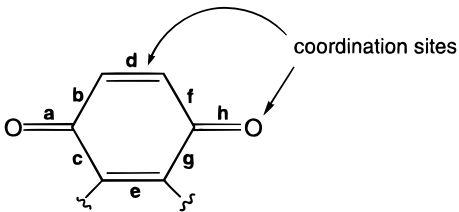
In Figure 3, the diffuse reflectance spectra of **1** and **2** are shown with that of Rh₂(O₂CCMe₃)₄. Rh₂(O₂CCMe₃)₄ shows two distinctive bands at 680 nm (band A) and 430 nm (band B). Band A has been assigned as the $\pi^*(\text{Rh}_2) \rightarrow \sigma^*(\text{Rh}_2)$

(7) Fair, C. K. *MolEN Structure Determination System*; Delft Instruments: Delft, The Netherlands, 1990.

(8) Cotton, F. A.; Felthouse, T. R. *Inorg. Chem.* **1980**, *19*, 323.

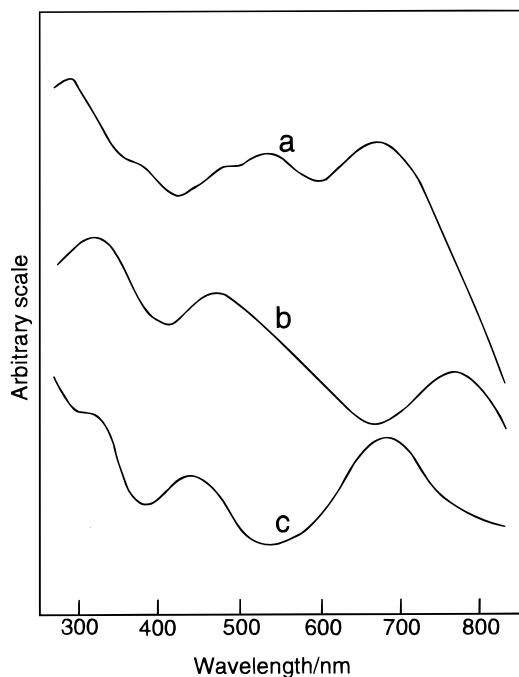
(9) Cotton, F. A.; Falvello, L. R.; Gerards, M.; Sntazke, G. *J. Am. Chem. Soc.* **1990**, *112*, 8979.

(10) (a) Trotter, J. *Acta Crystallogr.* **1960**, *13*, 86. (b) Gaultier, P. J.; Hauw, C. *Acta Crystallogr.* **1965**, *18*, 179.

Table 3. Bond Distances of the *p*-Quinone Moieties for **1** and **2** and Free 1,4-bq and 1,4-nq (Å)


complex	a	b	c	d	e	f	g	h	ref
1	1.219(7)	1.472(8)	1.468(6)	1.346(7)	1.326(7)	1.488(5)	1.452(7)	1.226(5)	this work
2	1.22(2)	1.47(2)	1.48(2)	1.37(1)	1.38(2)	1.45(2)	1.45(2)	1.22(1)	this work
1,4-bq	1.218(8)	1.467(6)	1.467(6)	1.312(8)	1.312(8)	1.467(6)	1.467(6)	1.218(8)	10a
1,4-nq ^a	1.21	1.48	1.43	1.31	1.39	1.45	1.46	1.22	10b

^a Estimated standard deviations for the bond lengths are not described in the literature.

**Figure 3.** Reflectance spectra of **1** (a), **2** (b), and $\text{Rh}_2(\text{O}_2\text{CCMe}_3)_4$ (c).

transition and band B as the $\pi(\text{Rh}-\text{O}) \rightarrow \sigma^*(\text{Rh}-\text{O})$ transition.^{2,11} In the corresponding visible regions, **1** and **2** have three absorption bands, respectively, *i.e.*, 480, 530, and 670 nm for **1** and 470, ca. 550 (the shoulder is obscure, but the spectral shape is indicative of this approximate absorption), and 760 nm for **2**. Since the position of band B is insensitive to the axial ligation, and since the $n \rightarrow \pi^*$ transition bands of 1,4-bq and 1,4-nq at 420–460 nm ($\epsilon < 35 \text{ mol}^{-1} \text{ dm}^3 \text{ cm}^{-1}$)¹² are much weaker than the B band ($\epsilon = 195 \text{ mol}^{-1} \text{ dm}^3 \text{ cm}^{-1}$ (in CH_2Cl_2) for $\text{Rh}_2(\text{O}_2\text{CCMe}_3)_4$), the band at 470–480 nm observed for both of the complexes can be assigned as the $\pi(\text{Rh}-\text{O}) \rightarrow \sigma^*(\text{Rh}-\text{O})$ transition. The other two bands might be assigned as the $\pi^*(\text{Rh}_2) \rightarrow \sigma^*(\text{Rh}_2)$ transitions. The band positions may be correlated with the strength of the axial interactions; there

are two types of Rh_2 units in the crystal: $//-(\text{Rh}-\text{Rh})-//$ and $\text{C}=\text{O}-(\text{Rh}-\text{Rh})-\text{O}=\text{C}$. However, it is strange that a band appears at 760 nm in **2**, because an axial interaction generally results in a blue shift of the $\pi^*(\text{Rh}_2) \rightarrow \sigma^*(\text{Rh}_2)$ transition band.¹³ The possibility of a significant bathochromic shift of the $n \rightarrow \pi^*$ transition band of the *p*-quinone perturbed by coordination (which may enhance the band strength) or of the appearance of the new band in this region due to the charge transfer between the *p*-quinone and the Rh_2 dimer cannot be excluded.

These complexes are soluble even in solvents with low solvating ability, such as benzene or dichloromethane. The absorption spectra of **1** and **2** were measured in dichloromethane. The spectral features are dependent on the concentration of the complexes. **1** has absorption bands at 420, 550, and 670 nm when the concentration is $1 \times 10^{-2} \text{ M}$. The band positions are almost identical to those observed in the reflectance spectrum. However, the spectral feature is quite similar to that of $\text{Rh}_2(\text{O}_2\text{CCMe}_3)_4$ when the concentration is $1 \times 10^{-3} \text{ M}$. Equilibrium between the dimer and the polymer species probably exists in the solution, which may be the reason for the concentration dependence of the spectrum. The concentration dependence of **2** was not as remarkable as that of **1**.

¹H-NMR spectra (in CDCl_3) have shown the concentration dependence of chemical shifts for the olefinic protons of the *p*-quinone for both the complexes: 6.82 ppm at $1 \times 10^{-3} \text{ M}$ and 7.02 ppm at $1 \times 10^{-2} \text{ M}$ for **1**; 7.04 ppm at $1 \times 10^{-3} \text{ M}$ and 7.28 ppm at $1 \times 10^{-2} \text{ M}$ for **2**. On taking into account that the free quinone molecules have the signals at 6.79 ppm for 1,4-bq and 6.99 ppm for 1,4-nq, the low-field shifts are small compared with the corresponding value for $\text{Rh}_2(\text{O}_2\text{CCF}_3)_4$ -((*-*)-*trans*-caryophyllene)₂, of which the signal for the olefinic proton is shifted from 5.2–5.4 ppm (free ligand) to 7.1 ppm (the complex). Furthermore, the ¹³C-NMR spectrum of **1**, which was measured in CDCl_3 at a concentration of $2 \times 10^{-2} \text{ M}$, showed that the chemical shifts of the carbonylic carbon (188.8 ppm) and the olefinic carbon (134.6 ppm) were almost identical to those of the free 1,4-bq molecule itself (187.0 ppm for the carbonylic carbon and 136.4 ppm for the olefinic carbon).¹⁴ These results reveal that the interactions of the carbonyl oxygens and the C=C double bonds of the quinones to the dimer are essentially weak.

The cyclic voltammograms (CVs) were measured for **1** and **2** in *o*-dichlorobenzene at a concentration of $1 \times 10^{-3} \text{ M}$. Two redox processes were observed in the reducing direction (for **1**, $E_{1/2} (= (E_{\text{pa}} + E_{\text{pc}})/2) = -0.44, -0.96 \text{ V vs SCE}$; for **2**, $E_{1/2} =$

- (11) (a) Trexler, J. W., Jr.; Schreiner, A. F.; Cotton, F. A. *Inorg. Chem.* **1988**, *27*, 3265. (b) Miskowski, V. M.; Schaefer, W. P.; Sadeghi, B.; Santarsiero, B. D.; Gray, H. B. *Inorg. Chem.* **1984**, *23*, 1154. (c) Felthouse, T. R. *Prog. Inorg. Chem.* **1982**, *29*, 73. (d) Boyar, E. B.; Robinson, S. D. *Coord. Chem. Rev.* **1983**, *50*, 109. (e) Jardine, F. H.; Sheridan, P. S. In *Comprehensive Coordination Chemistry*; Wilkinson, G., Ed.; Pergamon Press: New York, 1987; Vol. 4, p 944.
- (12) (a) Flaig, W.; Salfeld, J.-C.; Baume, E. *Ann. Chem.* **1958**, *618*, 117. (b) Singh, I.; Ogata, R. T.; Moore, R. E.; Chang, C. W. J.; Scheuer, P. J. *Tetrahedron* **1968**, *24*, 6053.

(13) Drago, R. S.; Long, J. R.; Cosmano, R. *Inorg. Chem.* **1981**, *20*, 2920.

(14) Berger, S.; Rieker, A. *Tetrahedron* **1972**, *28*, 3123.

−0.66, −1.05 V vs SCE) at the same potentials as the corresponding redox processes of each *p*-quinone molecule itself.¹⁵ New redox processes were detected at positive sides of the first reductions of the free quinones (−0.25 V vs SCE for **1** and −0.54 V vs SCE for **2**) at a concentration of 3×10^{-3} M, which may be due to an increase of the amount of the dimer species coordinated by the *p*-quinone molecules in the solution.

In summary, a novel coordination of the C=C double bond to the Rh₂ dimer has been found in the chain complexes $[\{\text{Rh}_2(\text{O}_2\text{CCMe}_3)_4(p\text{-Q})_2\}\{\text{Rh}_2(\text{O}_2\text{CCMe}_3)_4\}]_n$ (*p*-Q = 1,4-bq and 1,4-nq). The coordination of the C=C double bond and

the carbonyl oxygen is essentially weak, which leads to considerable dissociation of the quinone molecules from the dimers in the solution.

Acknowledgment. M.H. and M.M. are grateful for the financial support of a Grant-in-Aid for Scientific Research (Nos. 06740508 and 08404046) from the Ministry of Education, Science, Sports and Culture of Japan (Monbusho).

Supporting Information Available: Tables of atomic coordinates, isotropic and anisotropic thermal parameters, and bond lengths and angles and figures showing IR spectra in the carbonyl region and absorption spectra and CVs for **1** and **2** at various concentrations (17 pages). Ordering information is given on any current masthead page.

IC970246D

(15) Chambers, J. Q. In *The Chemistry of the Quinoid Compounds*; Patai, P., Ed.; John Wiley and Sons: London, 1974; p 737.